Eur. Phys. J. B **18**, 353–361 (2000)

THE EUROPEAN PHYSICAL JOURNAL B

EDP Sciences

Persistency of material element deformation in isotropic flows and growth rate of lines and surfaces

J. Duplat[1] and E. Villermaux[2,a]

[1] IUSTI, Technopôle de Château Goubert, 5 rue Enrico Fermi, 13453 Marseille Cedex 13, France
[2] IRPHE, Centre de Saint Jérôme, Service 252, 13397 Marseille Cedex 20, France

Received 10 November 1999 and Received in final form 14 August 2000

Abstract. We explore the consequence of isotropy on the growth of material lines and surfaces in complex flows. We show that the key parameter is the persistency $\gamma\tau$, defined as the product of a typical stretching rate γ to its associated coherence time τ. In particular, we derive the dependence of the net growth rate of both lines and surfaces on $\gamma\tau$. Their growth rates increase strongly with increasing persistencies for small $\gamma\tau$, and then saturate for $\gamma\tau \geq 10$. Making use of measurements of Girimaji and Pope [1], we estimate the persistency $\gamma\tau$ to be of order 1 in isotropic turbulence. We then comment on the evolution of the shape of an initially spherical material blob. While its length increases, one of its tranverse dimension increases slowly and the other one decreases. This quasi-two-dimensional deformation leads a final ribbon-shape.

PACS. 47.27.Ak Fundamentals – 47.27.Gs Isotropic turbulence; homogeneous turbulence – 47.27.Qb Turbulent diffusion

1 Introduction

Turbulent mixing is ruled by two complementary processes: the first of them is advection, possibly distributed over many scales in high Reynolds number flows and the second is diffusion responsible for the ultimate uniformization of the quantity being mixed (this is notably the case for the study of passive scalar mixing discussed in this paper, but this is also true for the mixing of the vorticity). Advection results in the reorganization of the spatial distribution of the scalar, inducing a reduction of the striation thickness [2], and enhancing large-scale dispersion, but keeping the intensity of segregation (a measure of the fine-scale uniformization of the mixture [3]) constant.

At the same time, rearrangements caused by advection increase local gradients in the scalar field and therefore accelerate the diffusion process. The rate of decrease of the scalar inhomogeneities is then fixed by the equilibrium between smoothing by diffusion and gradient production by advection-induced stretchings. It is therefore important to characterize the efficiency of this gradient production. We study here the deformation of simple material elements in a caricature of a turbulent flow, aiming at understanding, through the evolution of the dimensions of these elements, how stretching contributes to their deformation.

It is well known that in homogeneous isotropic turbulence material lines and surfaces grow in length and area. The stretchings experienced by the fluid elements in the course of their deformation, align material lines with the direction of maximum stretching, and material surfaces with the plane of the two directions of the maximum stretching, and this provided stretching is coherent for a sufficient long time (see *e.g.* [4]). In the case when perfect alignment is reached the growth rate of length and area are simply related to the eigenvalues of the deformation tensor. These eigenvalues are measurable through incompressibility and isotropy and the measure of the third moment of the longitudinal velocity spatial derivative [4].

Discussing incompressible flows, Cocke [5] and Orszag [6] consider the deformation due to a more complex history: they do not consider the effect of a single event, but the global evolution of material element due to cumulated stretchings in time. Cocke and Orszag summarize this history in a one deformation tensor, and by isotropic considerations show that lines and surfaces grow in a turbulent flow. No indication on the effective growth rates is given however, from their considerations. Cocke and Orszag results are very similar, both of them demonstrate the growth of lines and of surfaces independently, computing the effect of the advection on line and surface elements, and then averaging this effect on an isotropic distribution of the initial directions of these elements.

Kraichnan [7] relates the two growth rates. Through an assumption on the nature of the velocity field, he shows that the growth rates of lines and surfaces should be equal, but the assumption is not valid for isotropic turbulence. Kraichnan develops furthermore a model of white noise velocity field with short correlation time (*i.e.* in the limit where the coherence time tends to zero, but with

[a] e-mail: villerma@lrc.univ-mrs.fr

finite temporal auto correlation for the deformation tensor, the velocity field magnitude being taken inversely proportional to the square root of correlation time) for which he shows that lines should grow as a consequence of the dimensionality of space (for $d > 1$), but with a growth rate which can be equal to zero. However, Kraichnan also obtains that the mean growth rate of line elements (and also surface elements) is proportional to the temporal auto correlation of the deformation tensor, therefore underlying the role of the flow coherence time on the efficiency of the lengthening of line elements at least in the limit of small coherence times.

Between these two limits, namely the very long coherence time [4] and the very short coherence time [7] may lie real world turbulence. Numerical simulations [1] showed that the rate of growth of lines and surfaces are much smaller than the ones predicted by Batchelor and Townsend [4]. These authors [1] invoked a deficiency of coherence, arguing that the coherence is, in fact, much shorter than the one necessary to reach the asymptotic value of Batchelor and Townsend.

In this paper, we consider the effect of successive simple deformations on lines and surfaces. The velocity field in which the line element is embedded is fully characterized by the rate of the deformation tensor $\underline{e} = e_{ij} = \frac{\partial u_i}{\partial x_j}$, which can be decomposed into the sum of its symmetric part $\underline{\gamma} = (\underline{e}+{}^t\underline{e})/2$ and its antisymmetric part $\underline{\omega} = (\underline{e}-{}^t\underline{e})/2$ respectively the strain rate tensor, and the vorticity tensor. We define the intensity of the strain to be $\gamma = \sqrt{\gamma_x^2 + \gamma_y^2 + \gamma_z^2}$, where $(\gamma_x, \gamma_y, \gamma_z)$ are the eigenvalues of $\underline{\gamma}$, and the intensity of vorticity $\omega = \sqrt{\omega_x^2 + \omega_y^2 + \omega_z^2}$ to be the norm of the vorticity vector. We show that the final growth rate of lines and surfaces actually depends on the time coherence τ of each individual event, and more precisely on the persistency $\gamma\tau$, where γ denotes the stretching rate. Analytical results are provided in two dimensions, whereas in three dimensions we derive analytical bounds, a numerical integration giving interesting result in the special case where the ratio of the stretching rates of each axis is fixed and matches those obtained in grid turbulence [4].

We focus on the effect of stretching distribution isotropy, to recover the fact that lines and surfaces always grow, whatever the coherence time may be (which is the result of Cocke and Orszag) and we propose an estimation of the mean persistency in real flows through the comparison of our predictions with Girimaji and Pope simulation. At the Kolmogorov scale, $\gamma\tau \approx 1$ is found to be a good estimation. Because of dimensional constrains, we further argue that this result holds for any scale in the flow. The influence of vorticity is checked, and is found to be weak.

Finally, comparing the growth rate of lines and surfaces, we comment on the evolution of the shape of initially spherical material passive blobs. It is found that one transverse length is only weakly altered (it grows slowly), whereas the tranverse thickness decreases, and the length increases, leading finally a kind of a ribbon shape.

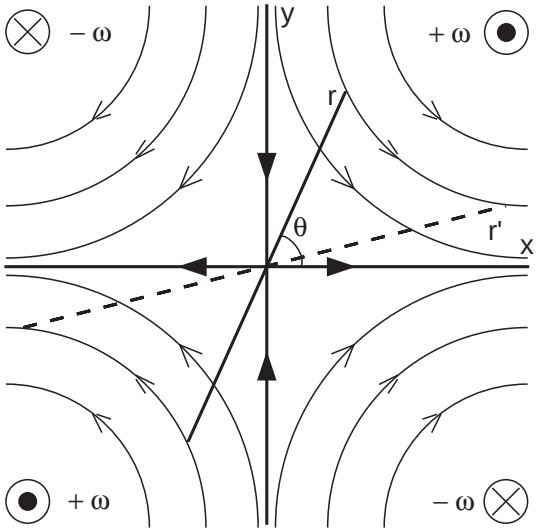

Fig. 1. Deformation of a line element in a 2D saddle point flow. The angle between the line element and the direction of stretching progressively goes to zero. The alignment time has to be compared to the coherence time of the saddle point flow to estimate the effective growth rate of the line.

2 Two-dimensional case

We are first interested in the stretching of a material line elements in a two-dimensional flow. We represent the flow as successive independent saddle points coherent on a time τ and on scale larger than the length of the line (Fig. 1), so that the deformation is uniform along the line for all times. The model can thus then be understood as a description of what happens in the regular range of scales in a turbulent flow, and for scales not affected by molecular diffusion *i.e.* larger than $\sqrt{D/\gamma}$ if D denotes the scalar diffusion coefficient. The model also describes the evolution of the separation distance between two fluid particles [8,9].

A saddle point flow is completely characterized by its two orthogonal main axes $\mathbf{x}$ and $\mathbf{y}$, and the rate $\gamma_x = \gamma/\sqrt{2}$ of stretching along the $\mathbf{x}$-axis (in an incompressible flow $\gamma_y = -\gamma/\sqrt{2}$). The extension of our results to a compressible flow is straightforward.

We first investigate one step of the construction of the line deformation: the element of line of initial length r is before the stretching at an angle θ from the $\mathbf{x}$-axis, so that its coordinates in the $(\mathbf{x}, \mathbf{y})$ axes are $(r\cos\theta, r\sin\theta)$ and become $(r\cos\theta\exp(\gamma_x\tau), r\sin\theta\exp(-\gamma_x\tau))$ after the stretching. The line has grown by a factor

$$r'/r\hat{E} = \sqrt{\cos^2\theta\exp(2\gamma_x\tau) + \sin^2\theta\exp(-2\gamma_x\tau)} \quad (1)$$

where r' stands for its final length. We see that the two important parameters which determine $\frac{r'}{r}$ are the initial angle θ and the product $\gamma\tau$, the latter being hereafter named *persistency*.

Note that in the compressible case, considering the dilatation rate $\gamma_{\rm d} = (\gamma_x + \gamma_y)/2$, and writing $\gamma'_x = \gamma_x - \gamma_{\rm d} = -(\gamma_y - \gamma_{\rm d})$ we have a growth factor of

$$r'/r\hat{E} = \exp(\gamma_{\rm d}\tau)\sqrt{\cos^2\theta\exp\left(2\gamma'_x\tau\right) + \sin^2\theta\exp\left(-2\gamma'_x\tau\right)} \tag{2}$$

which is the same as 1 but with an homotetic dilatation factor $\exp(\gamma_{\rm d}\tau)$.

Since we are interested in isotropic flows, the **x**-axis is isotropically distributed in space, whereas the intensity of the persistency is distributed independently, with a probability density function $P(\gamma\tau)$. After n steps (*i.e.* n consecutive isotropically distributed, independent stretchings) the line element has grown by a factor

$$\frac{r^{(n)}}{r^{(0)}} = \prod_{i=0}^{n-1}\frac{r^{(i+1)}}{r^{(i)}} = \left\langle\frac{r'}{r}\right\rangle_g^n \tag{3}$$

where the brackets $\langle.\rangle_g$ denote the geometrical mean, and $r^{(n)}$ denotes the length of the line after the nth step.

We have, assuming n is large enough so that the entire distribution $P(\gamma\tau)$ has been visited for all values of θ (remind that $\gamma = \sqrt{2}\gamma_x$),

$$\ln\left(\left\langle\frac{r'}{r}\right\rangle_g\right) = \int {\rm d}\gamma\tau P(\gamma\tau)\int_0^{2\pi}\frac{{\rm d}\theta}{2\hat{E}\pi} \times \ln\left(\sqrt{\cos^2\theta\exp\left(2\gamma\tau/\sqrt{2}\right) + \sin^2\theta\exp\left(-2\gamma\tau/\sqrt{2}\right)}\right). \tag{4}$$

The average over the isotropic distribution of the main axes of deformation can be split in the integral (4) and then exactly computed,

$$\ln\left(\left\langle\frac{r'}{r}\right\rangle_g\right) = \int {\rm d}\gamma\tau P(\gamma\tau) f(\gamma\tau) \tag{5}$$

with

$$f(\gamma\tau) = \frac{1}{2\hat{E}\pi}\int_0^{2\pi}{\rm d}\theta \times \ln\left(\sqrt{\cos^2\theta\exp\left(2\gamma\tau/\sqrt{2}\right) + \sin^2\theta\exp\left(-2\gamma\tau/\sqrt{2}\right)}\right) = \ln(\cosh(\gamma\tau/\sqrt{2})). \tag{6}$$

Since $f(\gamma\tau) = \ln(\cosh(\gamma\tau/\sqrt{2})) \geq 0$, lines grow within each class of $\gamma\tau$ and then whatever the persistency distribution $P(\gamma\tau)$ may be.

In a turbulent flow, stretchings are assumed to be due to eddies: an eddy of scale l with a characteristic velocity difference $\delta u(l)$ causes a stretching at rate $\gamma \sim \delta u(l)/l$. The coherence time of the stretching is related to the turnover time of the eddy $\tau \sim l/\delta u(l)$, so that the persistency $\gamma\tau$ is some constant C. The probability $P(\gamma\tau)$ is then centered around C, with some dispersion δC around the mean. We obtain a mean field result by considering that the persistency is monodispersed. The growth rate is then

$$\gamma_{\rm eff} = \ln(\left\langle\frac{r'}{r}\right\rangle_g)/\tau = f(C)/\tau = \gamma\ln(\cosh(C))/C. \tag{7}$$

It is proportional to the eigenvalue of the tensor deformation γ, through a multiplicative factor $\ln(\cosh(C))/C$ smaller than unity, but always positive (see Fig. 2).

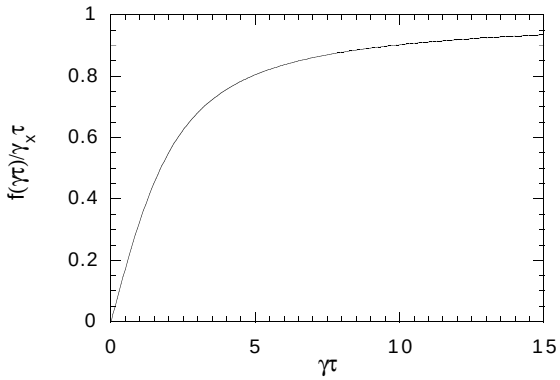

Fig. 2. Mean growth rate of a line in a 2D flow as a function of the persistency $\gamma\tau$. For large persistencies the effective growth rate of the line tends to the stretching rate of the saddle point flow. For small persistencies, it goes to zero.

The existence of a distribution of C around its mean results in a shift from the stretching rate expected in the absence of dispersion (*i.e.* for $\delta C = 0$). For a Gaussian distribution of coherence time (and for a fixed stretching rate γ), the shift is proportional to the curvature of $f(C)/C$ around the mean value:

$$\frac{\delta\gamma_{\rm eff}}{\gamma_{\rm eff}} = \frac{1}{2}\left(\frac{\frac{\partial^2 f(C)/C}{\partial C^2}}{f(C)/C}\right) \leq 0.35\left(\frac{\delta C}{C}\right)^2 \tag{8}$$

the maximal error being reached for $C = 2$ where the curvature of Figure 2 is maximum.

3 Three-dimensional case

We describe the flow stretchings by a set of consecutive stretching events defined by their three main axes of deformation **x**, **y**, and **z**, and their associated eigenvalues γ_x, γ_y and γ_z. For simplicity we still work in incompressible flows so that $\gamma_x + \gamma_y + \gamma_z = 0$. These events are distributed in intensity ($\gamma = (\gamma_x^2 + \gamma_y^2 + \gamma_z^2)^{\frac{1}{2}}$), in coherence time τ, in direction (the **x** direction of the stretching is taken isotropically distributed) and in aspect (the relative stretching rate along each direction is not fixed,

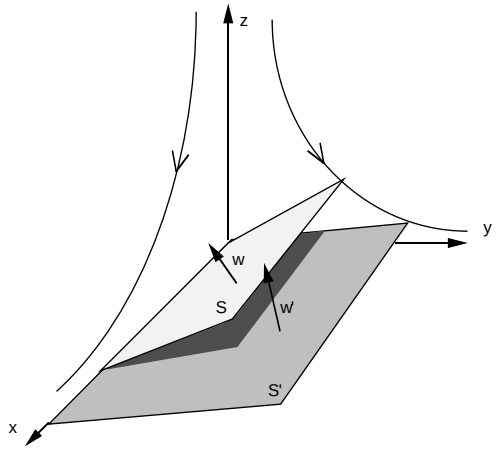

Fig. 3. Evolution of a surface in a 3D saddle point flow. The evolution of the "inverse thickness" $\mathbf{w}$ is imposed by the dual saddle point flow: the same main axes of stretching but with the opposite stretching rates.

the intermediate relative stretching rate γ_y/γ varies between $-1/\sqrt{6}$ and $1/\sqrt{6}$).

To follow the evolution of a plane surface, we follow the evolution of two non collinear vectors of this surface ($\mathbf{u}$,$\mathbf{v}$). The area of the total plane scales with the area of the parallelogram delimited by $(\mathbf{u}, \mathbf{v})$, provided the deformations are homogeneous all over the plane, which is the assumption of homogeneity of our model. We have

$$S \propto |\mathbf{w}| = |\mathbf{u} \wedge \mathbf{v}| \tag{9}$$

where S denotes the area of the surface element.

After a stretching, $\mathbf{u} = (u_x, u_y, u_z)$ becomes $\mathbf{u}' = (\mathrm{e}^{\gamma_x \tau} u_x, \mathrm{e}^{\gamma_y \tau} u_y, \mathrm{e}^{\gamma_z \tau} u_z)$ and so does $\mathbf{v} = (v_x, v_y, v_z)$ which becomes $\mathbf{v}' = (\mathrm{e}^{\gamma_x \tau} v_x, \mathrm{e}^{\gamma_y \tau} v_y, \mathrm{e}^{\gamma_z \tau} v_z)$. The vectorial product $\mathbf{w} = (w_x, w_y, w_z)$ becomes

$$\mathbf{w}' = \begin{pmatrix} \mathrm{e}^{\gamma_y \tau} \mathrm{e}^{\gamma_z \tau} (u_y v_z - u_z v_y) \\ \mathrm{e}^{\gamma_x \tau} \mathrm{e}^{\gamma_z \tau} (u_z v_x - u_x v_z) \\ \mathrm{e}^{\gamma_x \tau} \mathrm{e}^{\gamma_y \tau} (u_x v_y - u_y v_x) \end{pmatrix} = \begin{pmatrix} \mathrm{e}^{(\gamma_y + \gamma_z)\tau} w_x \\ \mathrm{e}^{(\gamma_x + \gamma_z)\tau} w_y \\ \mathrm{e}^{(\gamma_x + \gamma_y)\tau} w_z \end{pmatrix}. \tag{10}$$

The evolution of $\mathbf{w}$ (which describes the evolution of S) is the same as the evolution of a line element in the dual saddle point flow, defined by the same main axes $(\mathbf{x}, \mathbf{y}, \mathbf{z})$ but the eigenvalues $(\gamma_y + \gamma_z, \gamma_x + \gamma_z, \gamma_x + \gamma_y)$, equivalent to $(-\gamma_x, -\gamma_y, -\gamma_z)$ as a consequence of incompressibility (Fig. 3). We then see that the growth rate of the area S of a surface element is the growth rate of a line in the dual flow, and that the direct and dual flows are the image one of each other through symmetry of time, in incompressible flows.

The physical meaning of $\mathbf{w}$ is that its norm w is inversely proportional to the thickness e of a material sheet: by construction, $\mathbf{w}$ is in the direction tranverse to the sheet extent. Since w is proportional to S, we find, by mass conservation ($S \times e = \text{const.}$), that it is inversely proportional to e.

Consistently with an analogy proposed by Kraichnan [7], the growth of the surface area is the growth of its thickness in the dual flow. Kraichnan considers the evolution of hypersurfaces and lines in d dimensional flows. Under the assumption that any average of the velocity field is invariant under time reversal (in our vocabulary the flow is statistically auto-dual), he showed that lines and hypersurfaces grow at the same rate. We recover this result for $d = 3$, although we show here that the time reversal symmetry assumption is very restrictive, and that Kraichnan's result should be interpreted in this limit. The hypothesis of time reversal is notably not verified in the case of homogeneous turbulence (for instance the third moment of the velocity gradients at the dissipative scale is not zero, or as noted by Kraichnan himself, the transfer of energy dissipation function does not vanish).

According to the above remark, we can now restrict our analysis to the study of line elements. As in the two dimensions case, we will separate the effect of the distribution of the eigenvalues $(\gamma_x\tau, \gamma_y\tau, \gamma_z\tau)$, and the effect of the isotropic distribution of the main axes of the deformation tensor. We will also consider that the distribution of the eigenvalues is peaked around its most probable value.

We use the Euler angles (ψ, Ω, θ), ψ being the azimuthal angle between $\mathbf{z}$ and $\mathbf{r}$, Ω specifying the meridian of $\mathbf{z}$ and θ pointing $\mathbf{y}$ in the normal plane to $\mathbf{z}$ (we can choose $\theta = 0$ for $\mathbf{y}$ parallel to $(\mathbf{z} \wedge \mathbf{r})$). In this frame (see Fig. 4),

$$\mathbf{r}\hat{E} = (r\cos\theta\sin\psi, r\sin\theta\sin\psi, r\cos\psi)$$

becomes

$$\mathbf{r}' = (r\cos\theta\sin\psi\exp(\gamma_x\tau), r\sin\theta\sin\psi\exp(\gamma_y\tau), r\cos\psi\exp(\gamma_z\tau))$$

so that r'/r is independent of Ω. Averaging over an isotropic distribution of the line element $\mathbf{r}$ consists in integrating over ψ and θ with the normalized measure $\frac{1}{4\pi}\sin\psi \mathrm{d}\psi \mathrm{d}\theta$.

As in the two-dimensional case, we define an isotropic average growth rate within each class of constant persistency $(\gamma_x\tau, \gamma_y\tau, \gamma_z\tau)$,

$$f(\gamma_x\tau, \gamma_y\tau, \gamma_z\tau) = \int \frac{\mathrm{d}\theta \mathrm{d}\psi \sin\psi}{4\pi} \times \ln\left(\sqrt{(\mathrm{e}^{2\gamma_x\tau}\cos^2\psi + \sin^2\psi(\mathrm{e}^{2\gamma_y\tau}\cos^2\theta + \mathrm{e}^{2\gamma_z\tau}\sin^2\theta)}\right). \tag{11}$$

No analytical expression can be further derived, except in the special case where the deformation is axisymmetric, with two equal eigenvalues of the deformation tensor equal (for example $\gamma_y = \gamma_z = -\gamma_x/2$). In that case we get (see Fig. 5) for $\gamma_x \geq 0$

$$f(\gamma_x\tau, -\gamma_x\tau/2, -\gamma_x\tau/2) = \gamma_x\tau - 1 + \frac{\arctan(\sqrt{\exp(3\gamma_x\tau) - 1})}{\sqrt{\exp(3\gamma_x\tau) - 1}}, \tag{12}$$

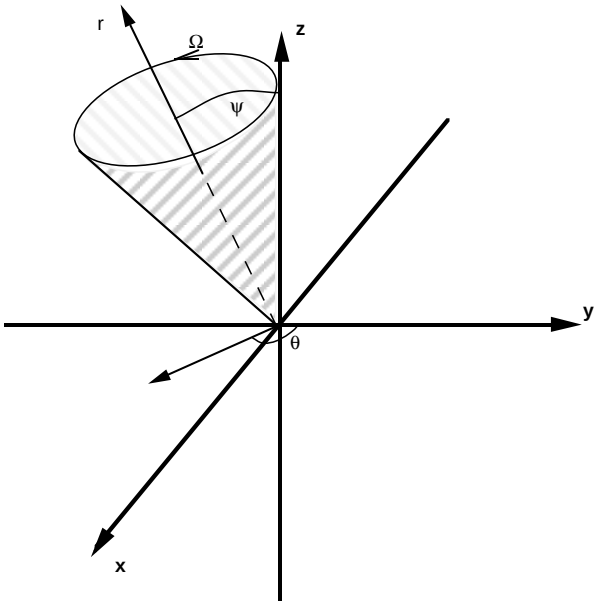

Fig. 4. Euler angles which define the main axes of deformation, for a given **r**.

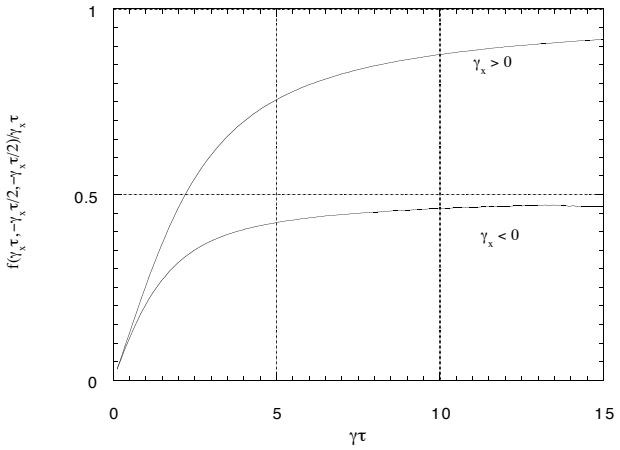

Fig. 5. Growth rate of a line in the axisymmetric case $(\gamma_x, -\gamma_x/2, -\gamma_x/2)$. As in the two-dimensional case, the growth rate of a line vanishes for small persistencies. In the limit of large persistencies, the line element is aligned with the direction of main stretching, and then grows at a rate fixed by this direction. In the axisymmetric case, whether there is one direction of stretching at a rate γ_x and two directions of compression, or there exists one direction of compression and two directions of dilatation at a rate $-\gamma_x/2$.

and for $\gamma_x \leq 0$

$$f(\gamma_x\tau, -\gamma_x\tau/2, -\gamma_x\tau/2) = \gamma_x\tau - 1 + \frac{\arg\tanh(\sqrt{1-\exp(3\gamma_x\tau)})}{\sqrt{1-\exp(3\gamma_x\tau)}}\,. \quad (13)$$

This case provides a lower limit for the growth rate: for some given persistency $\gamma_x\tau$ along the **x**-axis, the growth rate of lines is always larger than in the axisymmetric case $(\gamma_x\tau, -\gamma_x\tau/2, -\gamma_x\tau/2)$.

Indeed, introducing

$$g(\delta) = f(\gamma_x\tau, -\gamma_x\tau/2 - \delta/2, -\gamma_x\tau/2 + \delta/2) \quad (14)$$

with

$$\delta = -\gamma_y\tau - \gamma_x\tau/2 = \gamma_z\tau + \gamma_x\tau/2 \quad (15)$$

being the shift to the axisymmetric case, one has

$$\frac{\mathrm{d}}{\mathrm{d}\delta}g(\delta) = \int \mathrm{d}\psi\mathrm{d}\theta \sin^3\psi \times \frac{\exp(\delta)\cos^2\theta - \exp(-\delta)\sin^2\theta}{\mathrm{e}^{3\gamma_x\tau}\cos^2\psi + \sin^2\psi(\cos^2\theta\exp(\delta) + \sin^2\theta\exp(-\delta))} = h(\delta) - h(-\delta) \quad (16)$$

with

$$h(\delta) = \int \mathrm{d}\psi\mathrm{d}\theta \sin^3\psi \times \frac{1}{\mathrm{e}^{3\gamma_x\tau}\cos^2\psi + \sin^2\psi(1+\exp(-2\delta)\tan^2\theta)}\,. \quad (17)$$

The function $h(\delta)$ is increasing with δ and then $\left.\frac{\mathrm{d}g}{\mathrm{d}\delta}\right|_\delta$ is of the sign of δ. The function g thus presents a minimum for $\delta = 0$, which corresponds precisely to the axisymmetric case.

An upper limit of the growth rate is given by using the concavity of the logarithm (the logarithm of the mean is larger than the mean of the logarithms). We have

$$f(\gamma_x\tau, \gamma_y\tau, \gamma_z\tau) \leq \frac{1}{2}\ln(\frac{1}{3}(\exp(2\gamma_x\tau) + \exp(2\gamma_y\tau) + \exp(2\gamma_z\tau))). \quad (18)$$

We see that whatever the persistency of the stretching may be, lines and surfaces always grow, as demonstrated by Cocke [5], and that the growth rate lies between the two bounds 12 or 13 and 18. For a given value of f we deduce the growth rate of line and surfaces as

$$\gamma_{\mathrm{L}} = \frac{f(\gamma_x\tau, \gamma_y\tau, \gamma_z\tau)}{\tau} \quad (19)$$

for the line growth rate and

$$\gamma_{\mathrm{S}} = \frac{f(-\gamma_x\tau, -\gamma_y\tau, -\gamma_z\tau)}{\tau} \quad (20)$$

for the surface growth rate.

In order to apply this model to the context of turbulence, we make use of the mean eigenvalues of the stress tensor measured by Batchelor and Townsend [4]. These authors measured the third moment of the derivative of the longitudinal component of the velocity and deduced from the assumption of isotropy and incompressibility, the mean eigenvalues $(\gamma_x, \gamma_y, \gamma_z)$, and obtained

$$(\gamma_x, \gamma_y, \gamma_z) = \left(0.43\sqrt{\frac{\epsilon}{\nu}}, 0.12\sqrt{\frac{\epsilon}{\nu}}, -0.55\sqrt{\frac{\epsilon}{\nu}}\right) \quad (21)$$

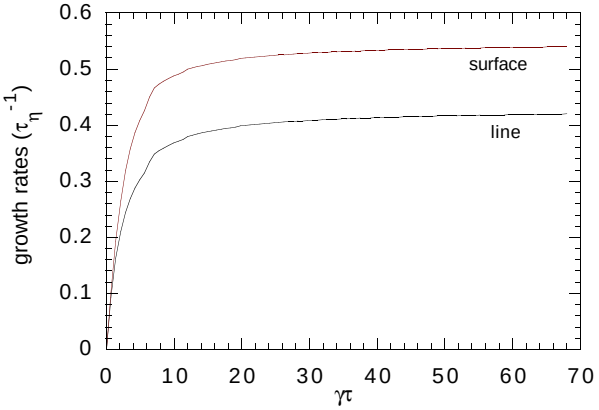

Fig. 6. Effective growth rate of lines (lower curve) and surfaces (upper curve) as a function of the persistency. In this case we chose $(\gamma_x, \gamma_y, \gamma_z) = (0.43\tau_\eta^{-1}, 0.12\tau_\eta^{-1}, -0.55\tau_\eta^{-1})$ for the stretching rates. With τ_η interpreted as a Kolmogorov timescale ($\tau_\eta = \left(\frac{\nu}{\epsilon}\right)^{\frac{1}{2}}$) these are the values measured by Batchelor and Townsend (1956) for the mean eigenvalues of the deformation tensor (and these are in good agreement with the Girimaji and Pope (1990) simulation).

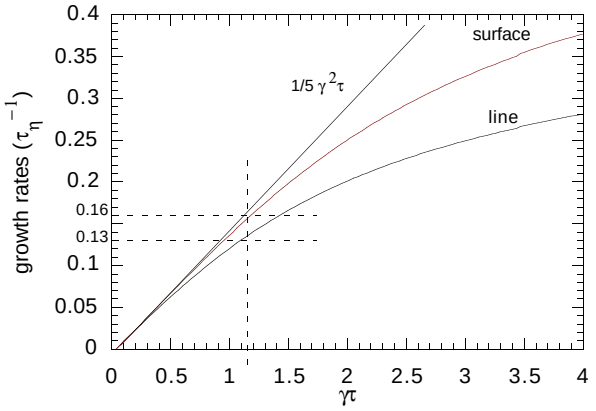

Fig. 7. Zoom of the Figure 6 for shorter persistencies. The values 0.13 τ_η^{-1} and 0.16 τ_η^{-1} are respectively the growth rates of lines and surfaces in Girimaji and Pope (1990) simulation.

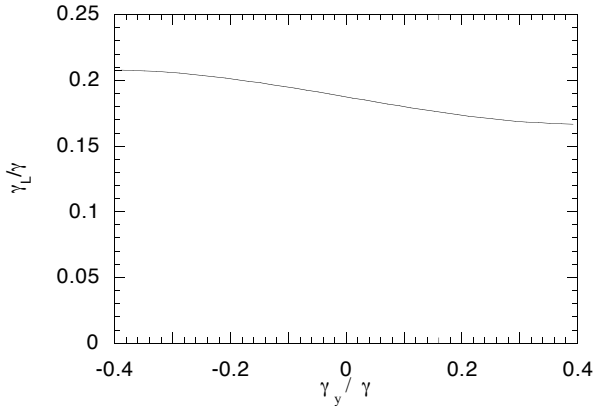

Fig. 8. Deformation geometry effect: the line growth rate depends on the deformation aspect ratio. For a persistency $\gamma\tau = 1$, this dependance is weak, and the growth rate varies between 21%γ for an axisymmetric deformation with one stretching direction, to 17%γ for an axisymmetric deformation with two stretching directions.

where ϵ is the viscous dissipation rate and ν the kinematic viscosity of the fluid. The scale associated with these deformations is of the order of the Kolmogorov scale.

As in two dimensions, we will consider the isotropic distribution only, neglecting the effect of the distribution of the persistency $\gamma\tau$, which is assumed to be peaked, and of the aspect ratio γ_y/γ. All the events are considered to be of the same persistency and of the same aspect. The aspect $\gamma_y/\gamma = 0.18$ is chosen to match the result of Batchelor and Townsend [4]. Ashurst *et al.* [10] computed from numerical simulations of homogeneous turbulence and shear flows the distribution of the aspect. It was found to depend on the intensity of the stretching: for small stretching intensities all aspects are possible whereas for more intensive stretchings the most probable aspect is found to be about $(3:1:-4)$ in quite good agreement with Batchelor and Townsend measurements.

We plot the numerically integrated value of γ_L and γ_S as a function of the persistency $\gamma\tau$ (Fig. 6). The asymptotic growth rate of lines $(0.43\sqrt{\frac{\epsilon}{\nu}})$ proposed by Batchelor and Townsend is nearly reached for persistencies $\gamma\tau \geq 10$.

Girimaji and Pope [1] measured in a (direct) numerical simulation of homogeneous, isotropic turbulence the mean eigenvalues of the deformation tensor and the mean growth rate of lines and surfaces. The deformation tensor was found to be about $(0.4\tau_\eta^{-1}, 0.1\tau_\eta^{-1}, -0.5\tau_\eta^{-1})$ with $\tau_\eta = \sqrt{\nu/\epsilon}$ being the Kolmogorov timescale, thus in good agreement with the measured value of Batchelor and Townsend [4]. The effective growth rate for lines and surfaces were found to be respectively $0.13\tau_\eta^{-1}$ and $0.16\tau_\eta^{-1}$. These values are appreciably smaller than the ones expected from the perfect alignment hypothesis. We recover independently the growth rate of lines and the growth rate of surfaces measured by Girimaji and Pope for persistency $\gamma\tau$ of about 1 (see Eqs. (19, 20) and Fig. 7).

We obtain here a mean result through a mean field theory, since neither the distribution of persistencies nor the distribution of stretching aspect ratio are taken into account. The correction due to persistency distribution is weak, as Figure 7 shows a very light curvature around $\gamma\tau = 1$. The geometrical distribution effects are more difficult to discuss. The growth rate of line γ_L as a function of the aspect ratio γ_y/γ for a constant γ (Fig. 8) and a persistency of 1 exhibits a weak dependence: the ratio of the effective growth rate to the intensity of stretching varies between 17% and 21%. It is 18% for the aspect ratio we select for our computation. The relative error induced by this choice on the estimation of the mean persistency is then of order one sixth.

4 The role of vorticity

Our model purposely ignores vorticity *i.e.* the antisymmetric part of the deformation tensor $\underline{\omega}$. We now come

to this point. In the absence of vorticity, the alignment of a line element with the direction of maximum stretching is due to stretching, and when perfect alignment is reached, the line grows at its maximal rate. A measure of the time $t_{\rm al}$ needed to reach this state is given by the time needed for the line effective growth rate to reach its asymptotic value. It is found that $\gamma t_{\rm al} \approx 2\sqrt{2}$ in two dimensions and $\frac{1}{5}\gamma^2 t_{\rm al} \approx \gamma_x$, that is $\gamma t_{\rm al} \approx 3$ in three dimensions. Therefore the average angular velocity of the line element solely due to stretching is about $\gamma/2\sqrt{2}$ in two dimensions and $\gamma/3$ in three dimensions. If now we consider a flow incorporating both stretching and vorticity, one sees that vorticity will have a negligible contribution as long as ω/γ is smaller than $1/2\sqrt{2}$ in two dimensions and $1/3$ in three dimensions.

A convincing example consists in choosing for the basic flow, instead of a pure saddle point, a shear flow where $v_x = 2\gamma_x y$ and $v_y = 0$ (in two dimensions). The eigenvalues of the rate of strain tensor are the same as those of the saddle point flow but now a pure rotation is superimposed (see *e.g.* [2]) so that $\omega/\gamma = 1$. This flow incorporates more vorticity than the threshold we derived heuristically above ($\omega/\gamma = 1/2\sqrt{2}$), but even in that case, the line growth rate $f(\gamma\tau)/\tau$ is identical to that of the saddle point flow for small persistencies ($\gamma\tau \to 0$) and is only 15% smaller for $\gamma\tau = 1$. The difference shows-up for persistencies larger than 3 (see Fig. 9).

The knowledge of the symmetric part of the deformation tensor $\underline{\gamma}$ is thus sufficient to estimate material line growth. The fact that the growth rate measured by Girimaji and Pope DNS are recovered within this assumption for both lines and surfaces at the same persistency of order unity is an *a posteriori* justification.

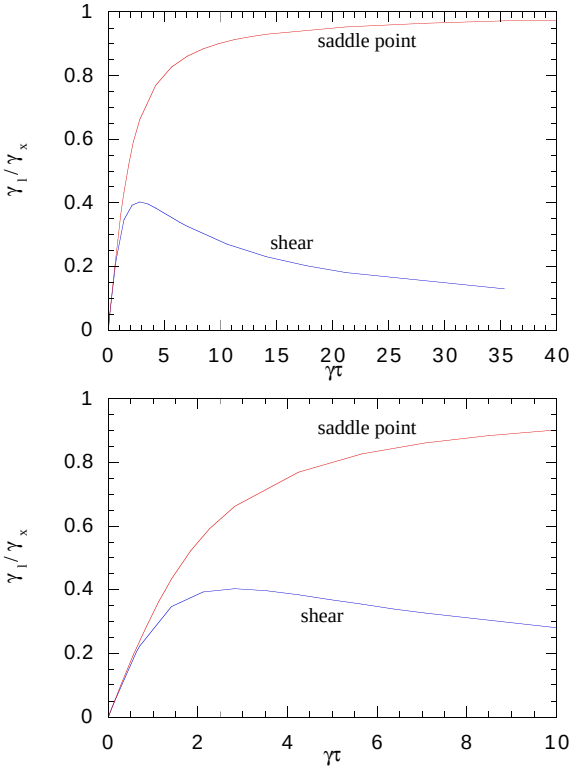

Fig. 9. Comparison of the line growth rate in two dimensions for the generic case of saddle point stretching (without vorticity) and for a shear flow (the vorticity being then as intense as the stretching). For relevant persistencies ($\gamma\tau \approx 1$), both cases are not significantly different: vorticity plays the poor rule in the growth of lines in turbulent flows. The bottom picture is a zoom of the upper one.

5 Evolution of the shape of initially compact blobs

The fact that surfaces grow does not necessary imply that an initial spherical "blob" immersed in a three-dimensional flow will form two-dimensional thin sheets.

To estimate the three characteristic dimensions of an object in the course of its cumulated stretchings, we simply need to compare the growth rate of lines, surfaces, and volumes. Indeed the evolution of the largest length of an object is given by the evolution of a line; the product of the two largest lengths gives the typical surface of the object and finally the product of the three largest lengths is a volume.

The typical dimensions (l_1, l_2, l_3) (see Fig. 10) of an object scale like $(\exp(\gamma_1 t), \exp(\gamma_2 t), \exp(\gamma_3 t))$ with $\gamma_1 = \gamma_{\rm L} = f(\gamma_x, \gamma_y, \gamma_z)/\tau$ (the growth rate of a line) and $\gamma_1 + \gamma_2 = \gamma_{\rm S} = f(-\gamma_x, -\gamma_y, -\gamma_z)/\tau$ (the growth rate of a surface).

It then appears that in the case of an isotropic flow, one of the transverse direction of the blob will vary much more slowly than the two other directions. Starting with an initial spherical blob of size l_0 we thus obtain a kind of ribbon with one direction much stretched, another one much compressed, the third direction remaining at a size of the order the initial size l_0 (Fig. 10).

The evolution of the shape of the blob is dictated by two parameters. One is the aspect of the deformations. If there are two axes of stretching we form pancakes (two-dimensional structures) as if there are two axes of compression we form cigars (one dimension filaments) – the nomenclature is from [1].

The other parameter is the persistency. For small persistencies indeed, lines and surfaces are found to growth at the same rate $(1/5)\hat{E}\gamma^2\tau$ (Eq. (3.3) for small $\gamma\tau$ gives $f \sim (1/5)\gamma^2\tau^2$). In this limit the final shape of the blob will be the ribbon shape. In the case we have studied and for a persistency of about 1, we obtain a final deformation aspect of $(0.13\tau_\eta^{-1}, 0.03\tau_\eta^{-1}, -0.16\tau_\eta^{-1})$, close to the asymptotic aspect of [4]. This distinguishes notably the short correlation model of Kraichnan [7] from the measurements of Girimaji and Pope [1].

6 Conclusion and further comments

We have shown how lines and surfaces grow under the simple effect of isotropically distributed stretchings, and we have shown the importance of the coherence time of these

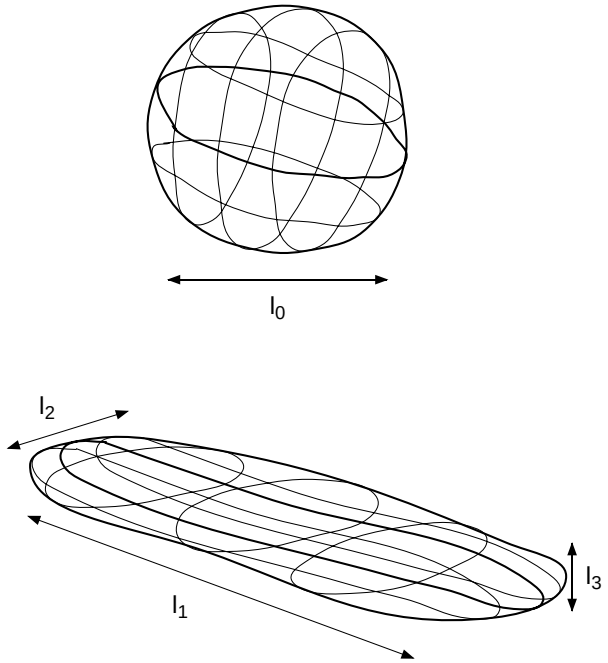

Fig. 10. Evolution of the shape of a blob element in time. From a spherical shape of characteristic size l_0, the blob becomes stretched in one direction, compressed in another, the third direction being nearly unchanged. The characteristic dimensions of the blob evolve as $l_1 \sim l_0 \exp(0.13t/\tau_\eta)$, $l_2 \sim l_0 \exp(0.03t/\tau_\eta)$, and $l_3 \sim l_0 \exp(-0.16t/\tau_\eta)$.

stretchings on the net growth rate. Comparison between our results and numerical simulations allowed us to give an estimation of the persistency: $\gamma\tau \approx 1$. This result is an average result since it is assumed in our model that all the stretchings in actual flows have the same persistency and that the relative rate of stretchings of deformation (what we called the aspect) is constant. We also take averaging over the number of stretchings (in our model) for time averaging (used in experiments and in DNS). This ergodic assumption becomes invalid if the coherence time τ is widely distributed.

To properly study the impact of the gap between real turbulent flow and our ideal model, it would be useful to measure these several distributions by Lagrangian statistics. However we have seen that the mean field model was reasonable, and allowed us the estimation of the persistency.

Turbulent flows present a hierarchy of scales: the statistics of the velocity fields exhibits a scale dependence such that the stretching rate observed at a scale r decreases as $r^{-\frac{2}{3}}$. This scale hierarchy is directly observable in the evolution of a material line. The total length of the line increases faster than the separation distance of its two extremities because of the rippling of the line [11,12]. The model we developed does not take into account this rippling and only describes the separation distance of the extremities of the line. The evolution of this separation distance was computed for constant persistency along the evolution, and with this assumption, the scale dependence of the stretching rate can be taken into account. The effective growth rate of the separation distance depends on the scale (with the same dependence than the stretching rate) and then it evolves algebraically in time $r \sim t^{\frac{3}{2}}$ [13]. This can be interpreted as an exponential growth in the number of events $r^{(n)}/r^{(0)} \sim \mathrm{e}^n$ (with $n = \sum_1^n \gamma_i \tau_i$), with events less and less intense, but lasting longer and longer ($\tau_i \sim r_i^{2/3}$). The time dependence $t = \sum_1^n \tau_i = \sum_1^n \mathrm{e}^{(2/3)i} \sim \mathrm{e}^{(2/3)n}$ is then dominated by the last event (the longer one), so that the number of events having occurred at time t is logarithmic ($n = (3/2)\ln t$) and that r grows algebraically ($\ln r = 3/2 \ln t$).

We explored the consequences of isotropy over scales larger than the line element. Strictly speaking we should then restrict ourselves to scales below the Kolmogorov scale, but the application of the model can be extrapolated to larger scales, as we only required that there exists some coherent flow that rules the dispersion of the two extremal points of the line (*i.e.* that the two points are within the same integral scale). Corrsin [14] studied the complementary case where the two points are separated by a distance larger than the integral scale. The statistics of the evolution of each particle are then independent one of each other. Under the assumptions that both of these statistics are isotropic, Corrsin showed that the separation distance grows, so that the extension of the line persists above the integral scale.

We have shown here that lines and surfaces grow in isotropic flows, so that even in the absence of molecular diffusion, we have a sign of the irreversibility of time. There is no strict need for the existence of a smallest scale in the flow, so that the model is still applicable to infinite Reynolds turbulence. The origin of the growth of line and then of the irreversibility is just related to the isotropy of the flow, and molecular diffusion plays no role in it.

Mixing, however is a matter of stretching enhanced diffusion. Considering the transient mixing of a scalar blob injected in a sustained turbulent flow, Villermaux *et al.* [15] show how the blob is first fragmented in structures of dimensions of the order of the Taylor scale and how these structures further experience stretchings so that their tranverse size decreases until it reaches the dissipation scale $\sqrt{D/\gamma}$, D being the diffusivity of the scalar. The resulting concentration probability density function presents an exponential tail (sharpening in time) and this is interpreted as the sign that all structures born at the same time have not the same history *i.e.* they have experienced different numbers of stretchings n. The transverse size of the initial blob is reduced little by little. Since we have shown that during a stretching event the tranverse size of the structure is reduced by a factor $\exp(-\gamma_S\tau)$ with $\gamma_S\tau = \frac{\gamma_S}{\gamma}\gamma\tau \approx \gamma_S/\gamma \approx 0.2$, and since the ratio between the dissipation scale and the initial scale is found experimentally to be $(5Sc)^{-1/2}$, the mean number of stretching events necessary to reach the dissipation scale is of order of 4 for temperature in air ($Sc = 0.7$), of 9 for temperature in water ($Sc = 7$), and of 23 for disodium fluorescein in water ($Sc = 2000$). These numbers appear to be sufficiently large so that the PDF of the number of stretchings

on a structure at a given time can be represented as Normaly distributed around its maximum as foreseen in [15].

References

1. S.S. Girimaji, S.B. Pope, J. Fluid Mech. **220**, 427 (1990).
2. J.M. Ottino, *The kinematics of mixing: stretching, chaos, and transport* (Cambridge University Press, 1989).
3. P.V. Danckwerts, Appl. Sci. Res. **A3**, 279 (1952).
4. G.K. Batchelor, A.A. Townsend, *Turbulent diffusion*, in *Surveys in Mechanics*, edited by G.K. Batchelor, R.M. Davies (Cambridge University Press, 1956) p. 352.
5. W.J. Cocke, Phys. Fluids **12**, 2488 (1969).
6. S.A. Orszag, Phys. Fluids **13**, 2203 (1970).
7. R.H. Kraichnan, J. Fluid Mech. **64**, 737 (1974).
8. B.L. Sawford, J.C.R. Hunt, J. Fluid Mech. **165**, 373 (1986).
9. P.A. Durbin, J. Fluid Mech. **100**, 279 (1988).
10. W.T. Ashurst, A.R. Kerstein, R.M. Kerr, C.H. Gibson, Phys. Fluids **30**, 2343 (1987).
11. S. Corrsin, M. Karweit, J. Fluid Mech. **39**, 87 (1969).
12. E. Villermaux, Y. Gagne, Phys. Rev. Lett. **73**, 252 (1994).
13. L.F. Richardson, Proc. R. Soc. Lond. A **110**, 709 (1926).
14. S. Corrsin, Phys. Fluids **15**, 1370 (1972).
15. E. Villermaux, C. Innocenti, J. Duplat, *Scalar fluctuation pdf's in transient turbulent mixing*, C.R. Acad. Sci. Paris, Sér. IIb **326**, 21 (1998).